Journal of Applied Physics ARTICLE scitation.org/journal/jap

Photothermal and spectroscopic characterization of Tb^{3+}-doped tungsten–zirconium–tellurite glasses

Cite as: J. Appl. Phys. **128**, 113103 (2020); doi: 10.1063/5.0020655
Submitted: 3 July 2020 · Accepted: 12 August 2020 ·
Published Online: 18 September 2020

J. F. M. dos Santos,[1,a)] V. S. Zanuto,[1] C. R. Kesavulu,[2] G. Venkataiah,[3] C. K. Jayasankar,[3] L. A. O. Nunes,[1] and T. Catunda[1]

AFFILIATIONS

[1]Instituto de Física de São Carlos, Universidade de São Paulo, Av. Trabalhador São-carlense 400, 13560-970 São Carlos, SP, Brazil
[2]SiC Laboratory, Centre for Materials for Electronics Technology (C-MET), Cherlapally, Hyderabad 500 051, India
[3]Department of Physics, Sri Venkateswara University, Tirupati 517 502, India

Note: This paper is part of the Special Topic on Photothermics.

[a)]**Author to whom correspondence should be addressed:** jessica.santos@usp.br. **Fax:** +55 16 33738093.

ABSTRACT

Among the glassy materials, tellurite glasses exhibit low phonon energy (~780 cm^{-1}), good mechanical stability, chemical durability, and high linear and nonlinear refractive indices, with a wide transmission window (typically 0.4–6.0 μm), which make them promising materials for photonic applications. In this work, tungsten–zirconium–tellurite glasses doped with several Tb^{3+} concentrations (0.1–4.0 mol. % Tb_2O_3) were prepared and characterized through absorption, emission, excitation spectra and fluorescence decay rate measurements. Only the green/yellow emission due to the $^5D_4$ level was observed since the $^5D_3$ was not observed in either the absorption or emission spectra due to cutoff absorption of the host matrix at ~470 nm. A concentration quenching effect was observed in the 545 nm green emission ($^5D_4 \rightarrow {}^7F_5$) with a critical Tb^{3+} concentration of 6.2×10^{20} cm^3 (1.7 mol. %). Thermal lens (TL) was performed in order to determine the thermo-optical properties of the glass such as thermal diffusivity ($D \sim 3.3\times10^{-3}$ cm^2/s) and optical path temperature coefficient ($ds/dT \sim 2.5\times10^{-5}$ K^{-1}). The energy transfer efficiency from the host matrix to the Tb^{3+} was estimated from excitation spectra as ~3%, in agreement with TL measurements which indicate that nearly all absorbed energy is converted into heat for 488 nm excitation ($^7F_6 \rightarrow {}^5D_4$). Z-scan measurements in the cw regime indicate a dominant thermal nonlinearity in agreement with TL data. However, the fluorescence measurements in the Z-scan indicate a strong saturation of the green fluorescence attributed to the effect of excited state absorption.

I. INTRODUCTION

Trivalent rare-earth (RE) ions present intense visible emission as a consequence of 4f → 4f transitions which are little sensitive to the ion's surrounding crystalline field due to the shielding effect of outer 5s and 5p shell electrons.[1] Consequently, these transitions have been studied aiming applications as phosphors, scintillators, lasers, and optical amplifiers, up and down conversion devices, etc. Among the rare-earths, Tb^{3+} is interesting mainly due to blue and green emissions with high fluorescence quantum efficiency.[2–6] Moreover, Tb^{3+}-doped glasses, with low phonon energy such as chalcogenide and telluride and wide transparence window, are important for mid-infrared emission from the $^7F_4$.[7] Recently, efficient cw lasing with the Watt level of output power in the green and yellow lines was obtained with Tb^{3+}-doped crystals,[8] but efficient laser action in glasses and fibers is still a challenge.[9] In fact, excited-state absorption (ESA) is a major loss mechanism that limited the laser action only in wide bandgap materials ($E_g > 5$ eV). Saturation of the green emission was observed in aluminosilicate glasses at pump intensities in two orders of magnitude lower than expected for bleaching of the ground state absorption.[2,3] In the same material, strong nonlinear heat generation was observed and attributed to ESA cross section ~2 orders of magnitude higher than the ground state absorption ($^7F_6 \rightarrow {}^5D_4$) at ~488 nm.[10]

Tellurite glasses present interesting physical and optical properties, such as low phonon energy (~780 cm^{-1}), good mechanical stability, chemical durability, and high linear and nonlinear refractive indices, with a wide transmission window (typically 0.4–6.0 μm). Typical host media (insulators with wide bandgap) have limited influence in the RE due to the effective screening of 4f

electrons by the outer shells. However, in the case of telluride glasses, the intra-4f-shell transition of RE dopant may overlap intrinsic transitions of the host.[11,12] ESA spectroscopy of Er^{3+} and Tm^{3+}-doped gallium lanthanum sulfide (GLS) chalcogenide glasses showed that highly excited RE energy levels are not affected by the host material in spite of its low $E_g = 2.6$ eV (transparence cutoff at ~500 nm). Thermal lens (TL) measurements were performed also in GLS host, but Nd^{3+}-doped, in order to determine the quantum efficiency of energy transfer (ET) from the host glass to RE ion ($\eta \sim 40\%$).[13] In fact, ET from host to RE has been observed in many semiconductors and chalcogenide glasses.[12] For instance, an efficient cooperative energy transfer mechanism, $Te^{4+} \rightarrow Yb^{3+}$, was observed in tellurite glasses.[14] Also, the high refractive index of tellurite is an important feature; for instance, it is generally known that materials with large linear refractive index also present high nonlinear refraction coefficient, n_2. Varying the glass modifiers (Nb_2O_5, Bi_2O_3, and TiO_2), Santos *et al.*[15] observed an increase in n_2 with the decrease of tellurite glass energy gap. The effect of silver nanoparticles was studied by ultrafast z-scan measurements in TeO_2-Zn glasses.[16] Moreover, resonant laser-induced refractive index changes can be observed in the cw regime due to the promotion of the RE ion to a metastable state. This effect is known as Population Lens (PL) and is attributed to the polarizability difference, between excited and ground states.[17–20] In the case of Nd^{3+}-doped glasses, it was observed that $\Delta\alpha_p$ varies one order of magnitude depending on the host material (crystal or glass). Usually material with large refractive index and small bandgap presents large $\Delta\alpha_p$ as shown by recent results in Nd^{3+}-doped tellurite[21] and Tb^{3+}-doped aluminosilicate glasses.[19] In this paper, we report absorption, emission, excitation spectra and fluorescence decay measurements of Tb^{3+} doped zinc tellurite glasses. The UV–Vis 4f–4f transitions of Tb^{3+} and the glass matrix absorption are strongly overlapped so only the green/yellow emission from the $^5D_4$ state could be observed. Moreover, TL and Z-scan measurements in the cw regime were also performed in order to investigate the thermo-optical properties and the PL effect. The results indicated a predominance of the thermal effect over the electronic contribution to the refractive index change mainly due to the host matrix background absorption. Both Z-scan and spectroscopic measurements indicate weak energy transfer from the host matrix to the doping Tb^{3+} ions. A saturation of the green emission was observed at low intensities, two orders of magnitude smaller than expected by bleaching of the ground state population. A strong effect of ESA to the 4f5d levels of Tb^{3+} is a possible explanation for this behavior, as previously reported for Tb^{3+}-doped materials.[2,9]

II. MATERIAL AND METHODS

The tungsten–zirconium–tellurite (TWZ) glasses were produced in the following molar composition: $70TeO_2 + (25 - x)WO_3 + 5ZrO_2 + x\ Tb_2O_3$, where $x = 0.1$, 0.5, 1.0, 2.0, and 4.0 mol. %. The samples were prepared by a melt, sudden quenching, and casting technique. Batch composition of 30 g of homogeneous mixture was melted at 900 °C for 1 h in an electric furnace using a platinum crucible. The melt was cast on to a preheated brass mold and pressed with another brass plate to get a flat disk of 2 mm thickness and then annealed at 330 °C for 12 h in order to release thermal strain and stress inside the glass samples. The obtained glasses were cut and polished for their spectroscopic measurements.

The absorption spectra of the samples were measured with a UV-vis-near infrared double beam spectrophotometer (Perkin-Elmer Lambda 900) in the spectral range of 400–800 nm. The excitation, emission, and decay curve measurements were carried out with a Jobin YVON Fluorolog-3 spectrofluorimeter with the xenon lamp as a light source in continuous as well as in pulsed modes.

A. Thermal lens technique

The TL technique is applied to study the modulation of the refractive index caused by thermal-optical effect. The TL effect occurs by deposition of heat (non-radiative process) after laser energy has been absorbed by the sample, causing the thermal expansion and a refractive index gradient in the medium. This transversal phase shift produced is given by[18,22,23]

$$\theta = -\frac{P_{abs}}{\lambda K}\varphi\frac{ds}{dT}, \tag{1}$$

where φ is the fraction of light-to-heat converted, $P_{abs} = P\alpha L$ is the absorbed excitation power, K is the thermal conductivity, λ is the wavelength of the probe beam and, ds/dT is the temperature coefficient of the optical path length. The fluorescence quantum efficiency (η) is related with the φ parameter through the relationship[23]

$$\varphi = 1 - \eta\frac{\lambda_{ex}}{\langle\lambda_{em}\rangle}, \tag{2}$$

with λ_{ex} being the excitation wavelength and λ_{em} being the weighted mean of the emission wavelengths. The characteristic TL response time (t_c) obtained from experimental data is associated with the thermal diffusivity (D), as shown below:

$$t_c = w_e^2/4D, \tag{3}$$

where the excitation beam radius at sample position.

The time-resolved mode-mismatched configuration was applied using an Ar^+ laser at $\lambda_{ex} = 488$ nm and a He-Ne laser at 632.8 nm as a probe beam of the TL effect. The fix experimental geometrical parameters $m = 26$ and $V = 4.8$ were used to fit the experimental data, as described in detail in Refs. 18 and 22.

B. Z-scan technique

The time-resolved Z-scan method[18,21,22] was applied to study 1.0 mol. % Tb^{3+}-doped tellurite glass with $\tau = 490\,\mu$s. The Z-scan measurements were performed by chopping the cw Ar^+ laser (488 nm) at the frequency $f = 500$ Hz, with initial time acquisition $t_i = 20\,\mu$s, final time acquisition $t_f = 750\,\mu$s, and aperture factor $S = 0.3$. Further details of the experimental arrangement can be found in Refs. 18 and 24.

III. RESULTS AND DISCUSSION

Figure 1 shows the partial energy level of Tb^{3+} ions in the energy range up to 40×10^3 cm^{-1} above the $4f^8$ ground state multiplet $^7F^6$ and selected radiative transitions. The energy levels of the

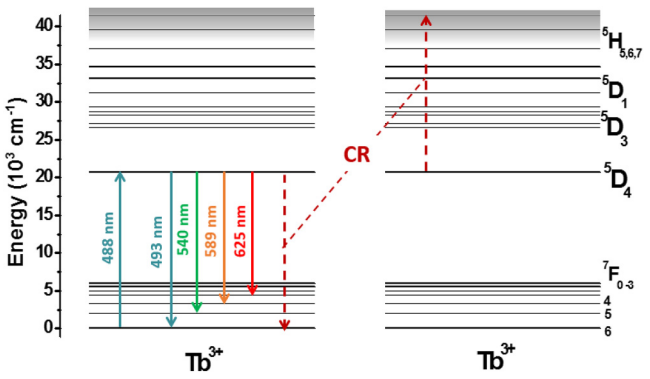

FIG. 1. Partial energy level diagram of Tb^{3+}-doped TWZ glasses. Colored arrows indicate radiative transitions. The dashed red arrows represent a cross-relaxation (CR) process.

$4f^8$-configuration of Tb^{3+} are rather complex. This situation strongly favors to energy transfer processes. In particular, the resonant cross relaxation (CR) efficiently quenches the $^5D_{3,4}$-fluorescence at high doping levels.[5,6,25–27]

A. Optical absorption spectra

Figure 2 shows the optical absorption spectra of undoped and 4.0 mol. % of Tb^{3+}-doped TWZ glasses recorded in the 450–825 nm spectral range along with the assignments of absorption bands. The broad peak at 656 nm is associated with host band of TWZ glasses. Only the line at 489 nm is attributed to Tb^{3+} ($^7F_6 \rightarrow {}^5D_4$ transition). This absorption line was analyzed subtracting the background absorption due to the host, as shown in the inset. We verified that this absorption area increases linearly with the Tb^{3+} concentration. The absorption cross section (σ) at peak wavelength was calculated, $\sigma = 3.9 \times 10^{-22}$ cm^2 using the nominal Tb content. This value is expected to be small since all transitions from the $^5D_4$-multiplet are spin and parity forbidden.

B. Excitation and emission spectra

Figure 3 shows the excitation spectrum of 1.0 mol. % Tb^{3+}-doped TWZ glass measured by monitoring the green emission of Tb^{3+} ions at 540 nm. As can be seen from Fig. 3, the two transitions $^7F_6 \rightarrow {}^5D_3 + {}^5G_6$ (~378) and $^7F_6 \rightarrow {}^5D_4$ (489 nm) are attributed to Tb^{3+} ion excitations. It should be noticed that the main 489 nm peak is over a plateau, which indicates ET from the host matrix to the Tb^{3+} ion. However, this ET is not effective since the signal due to the resonant line is ~4 times higher than the plateau. This relation does not follow the same trend observed in Fig. 2, where the host background absorption (~0.82 cm^{-1}) is 5.5 times higher than the ion absorption (~0.15 cm^{-1}). From these numbers, we estimate that at 488 nm only 3.2% of absorbed photons from the host glass results in the excitation of $^5D_4$ state of Tb^{3+}. This indicates that the ET from the tellurite host to Tb^{3+} is very inefficient and the most of absorbed energy should be converted into heat.

The emission mechanism of Tb^{3+} ions in TWZ glasses was studied through 455 nm excitation (or $E_{exc} \sim 2.7$ eV), corresponding to the $^7F_6 \rightarrow {}^5D_4$ transition (see Fig. 1). The emission bands with peak maxima at around 493, 540, 589, and 625 nm have been assigned to the $^5D_4 \rightarrow {}^7F_6$, $^5D_4 \rightarrow {}^7F_5$, $^5D_4 \rightarrow {}^7F_4$, and $^5D_4 \rightarrow {}^7F_3$ transitions, respectively, as shown in Fig. 4. Among these, the $^5D_4 \rightarrow {}^7F_5$ transition has considerably strong intensity compared to other transitions. It is observed that the emission intensities of $^5D_4$ state increase with increasing Tb^{3+} ion concentration for all the samples (Fig. 4).

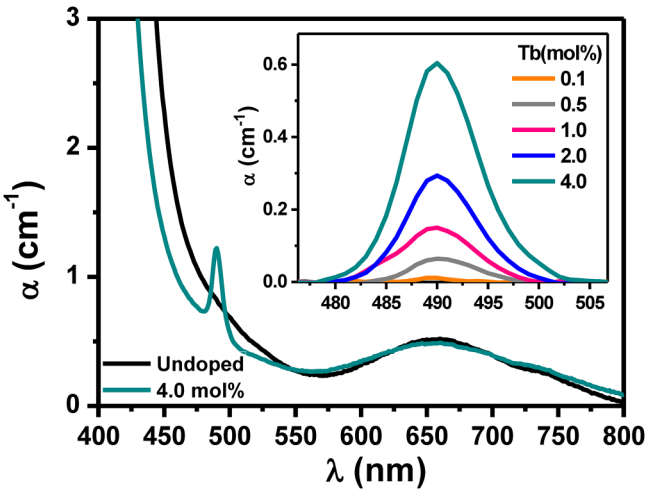

FIG. 2. Absorption spectra of undoped glass and 4.0 mol. % Tb^{3+}-doped TWZ glass. The inset shows the $^7F_6 \rightarrow {}^5D_4$ absorption transition of Tb^{3+} ions.

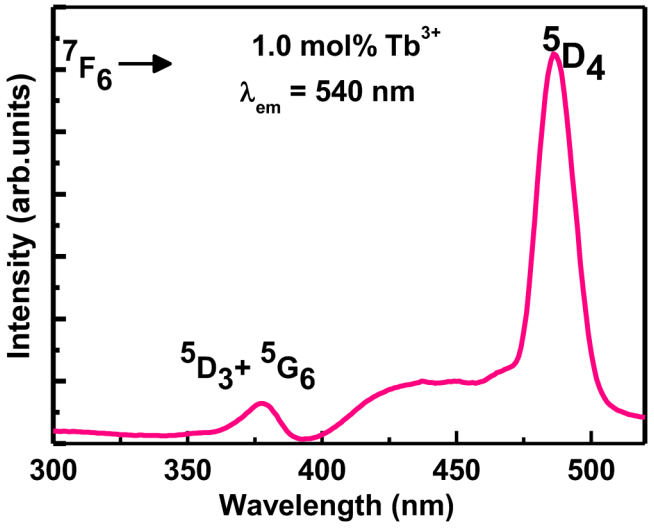

FIG. 3. Excitation spectrum of 1.0 mol. % Tb^{3+}-doped TWZ glass, $\lambda_{em} = 540$ nm.

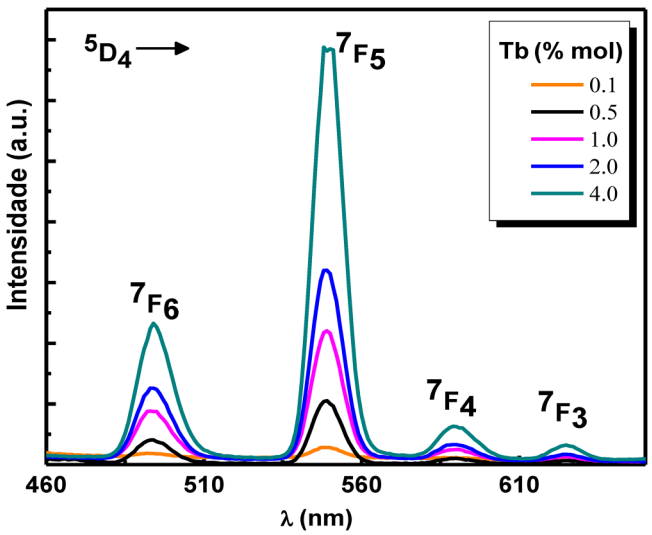

FIG. 4. Emission spectra of Tb^{3+}-doped TWZ glasses (λ_{ex} = 455 nm).

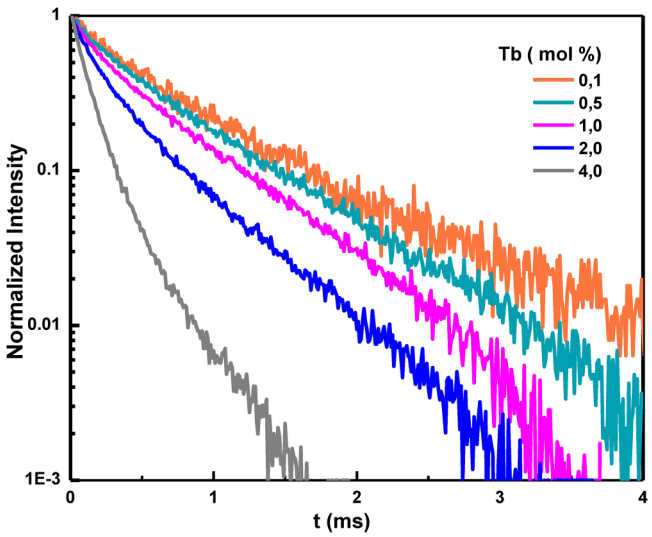

FIG. 5. Decay curves for the $^5D_4$ level of TWZ glasses for different Tb^{3+} ion concentrations under 488 nm excitation.

C. Fluorescence decay curve analysis

The fluorescence decay analysis of an emission level is more useful to know the luminescence quenching and energy transfer among the excited Tb^{3+} ions, if any. The fluorescence decay curves of the $^5D_4$ emission level of Tb^{3+} in TWZ glasses are recorded by exciting at 488 nm wavelength and monitoring the emission at 540 nm. The logarithmic plots of the fluorescence decay profiles of TWZ glasses are presented in Fig. 5. The fluorescence decay profiles (Fig. 5) are well fitted by a single exponential only for concentrations lower than 1.0 mol. %. At higher concentrations, fluorescence decay curves have the nonexponential character, so the effective lifetimes were obtained by integration of the fluorescence signals.[2] This effect is reported in the literature[6,28] and is attributed to the CR process, $^5D_4 \sim {}^7F_6/{}^5D_4 \sim$ Upper laying levels (UL), as indicated in Fig. 1. The effective values are determined to be 0.63, 0.58, 0.49, 0.34, and 0.13 μs for 0.1, 0.5, 1.0, 2.0, and 4.0 mol. % Tb^{3+}-doped glasses, respectively.

The decrease of decay time with the increase of ion concentration is known as lifetime quenching and is usually analyzed with the following empirical formula:[1]

$$\tau_{exp} = \frac{\tau_0}{1 + (\frac{N}{Q})^p}, \quad (4)$$

where τ_o is the luminescence lifetime in the limit of zero concentration, N is the Tb^{3+} ion concentration, Q is the concentration quenching, and p is the phenomenological parameter characterizing the steepness of the corresponding quenching curve. The fit in Fig. 6 shows the dependence of $^5D_4$ lifetime as a function of Tb^{3+} ions concentration up to 6.0 mol. % of Tb^{3+}. The fit by Eq. (4) results in $\tau_o = (730 \pm 20)\,\mu$s, $Q = (1.7 \pm 0.1)$ mol. %, and $p = 1.7 \pm 0.2$. This $p \sim 1.7$ value is close to 2, as expected for a CR mechanism. In the case of the $^5D_4$ decay of Tb^{3+}, the CR process is shown in Fig. 1. The $Q = 1.7$ mol. % corresponds to 6.2×10^{20} ions/cm^3. The decrease of excited-state decay time is related to the reduction of quantum efficiency, $\eta = \tau_{exp}/\tau_0$. The calculated η values are present in Table I.

D. TL measurements

Figure 7 presents a typical normalized TL transient signal for the 1.0 mol. % doped glass under the excitation of 488 nm of the

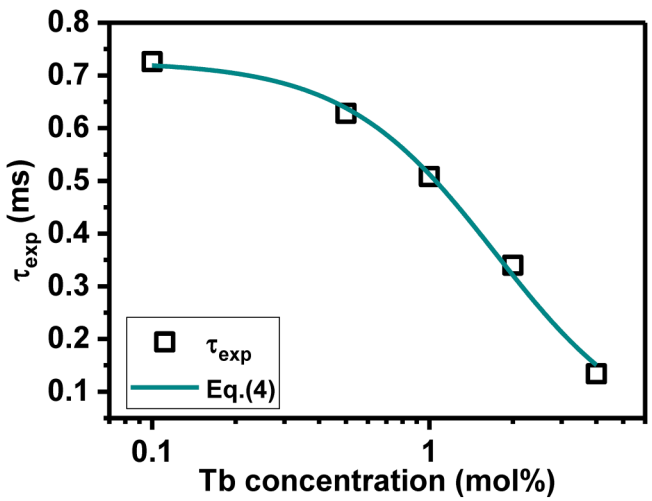

FIG. 6. Tb^{3+} concentration dependence of the $^5D_4$ decay time (τ_{exp}). The green solid line represents the fitting results using Eq. (4).

TABLE I. Spectroscopic and TL parameters for Tb^{3+}-doped TWZ glasses.

Tb^{3+} (mol. %)	Tb^{3+} ($\times 10^{20}$ cm^{-3})	L (mm)	η	$<t_c>$ ($\times 10^{-3}$ s)	θ/P_{ab} (rad/W)	K ($\times 10^{-3}$ cm^2/s)
0.1	0.37	2.33	0.99	1.14 ± 0.02	21.3 ± 0.2	7.6 ± 0.3
0.5	1.83	2.16	0.86	1.17 ± 0.03	20.1 ± 0.3	7.4 ± 0.2
1.0	3.65	2.38	0.63	1.11 ± 0.02	22.8 ± 0.2	7.8 ± 0.2
2.0	4.25	2.59	0.46	1.10 ± 0.03	22.8 ± 0.2	7.8 ± 0.2
4.0	14.22	2.12	0.18	1.19 ± 0.04	22.4 ± 0.3	7.4 ± 0.2

Ar^+ laser, in resonance with the $^7F_6 \rightarrow {}^5D_4$ absorption of Tb^{3+} (Fig. 1). The signal increase in Fig. 7 reveals a convergent character of the induced thermal lens signal ($ds/dT > 0$), similarly to other tellurite glasses.[21,29] The solid line represents the theoretical fit,[18,21] which provides two parameters: θ and the characteristic TL response time, t_c. The fit results are $\theta = (6.20 \pm 0.02) \times 10^{-2}$ rad and $t_c = (1.00 \pm 0.01) \times 10^{-3}$ s. Transient signals were taken as a function of P up to ~50 mW, as shown in Fig. 8. The linear increase of θ vs P was observed, in all Tb^{3+}-doped TWZ samples, as expected by Eq. (1). The t_c values remained approximately constant with a relative error lower than 5%.

Figure 9 shows that D is nearly constant for different Tb^{3+} concentrations in TWZ glasses. The average value $D = (3.3 \pm 0.1) \times 10^{-3}$ cm^2/s is similar to that obtained in others tellurite glasses.[21,29,30]

The thermal conductivity can be obtained from the experimental D values using the relationship $K = \rho CD$, where ρ is the density and C is the specific heat. Therefore, using $\rho C = 2.3$ J/K cm^3 (Ref. 21) obtained in a similar glass matrix, $K \sim 7.6$ W/K cm was estimated.

To determine the φ value by a blue photon absorption ($\lambda_{ex} = 488$ nm) in Tb^{3+}-doped TWZ glasses, some considerations need to be made. In fact, the $^5D_4$ state of Tb^{3+} ions can be directly excited by the Ar^+ laser ($\lambda = 488$ nm), close to the peak at 489 nm ($^7F_6 \rightarrow {}^5D_4$). Indeed, Fig. 2 shows that the TWZ host matrix absorption is greater than the absorption due to Tb^{3+} ions. For instance, for the 1.0 mol. % Tb^{3+}-doped TWZ, the glass absorption $A_{TWZ} \sim 0.4$ cm^{-1} is nearly three times greater than the Tb^{3+} absorption. Moreover, from the excitation spectrum, we estimated that most of absorbed energy at 488 nm should be converted into heat, so we expect $\varphi \sim 1$. In fact, Table I shows that the experimental data $\theta/P_{abs} \sim (22 \pm 1)$ are nearly independent of the Tb^{3+} concentration, corroborating that the TL should be attributed only to the glass matrix absorption. Therefore, from Eq. (1) we obtained $ds/dT \sim 2.5 \times 10^{-5}$ K^{-1}.

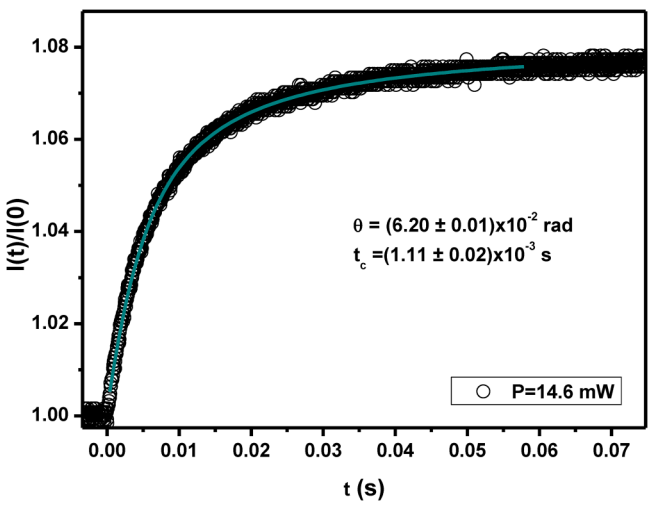

FIG. 7. TL transient signal for $P_{ex} = 14.6$ mW, $\lambda_{exc} = 488$ nm, and $\lambda_p = 632.8$ nm. The solid line corresponds to the theoretical fit provided in Ref. 18. The curve fitting provides $\theta = (6.20 \pm 0.02) \times 10^{-2}$ rad and $t_c = (1.11 \pm 0.01) \times 10^{-3}$ s for 1.0 mol. % of Tb^{3+}-doped zinc telluride glass.

E. Z-scan analysis

Closed aperture Z-scan experiments were performed in the undoped and 1 mol. % Tb^{3+}-doped zinc tellurite glasses, as shown in Figs. 10(a) and 10(b), respectively. The measurements were performed using an Ar^+ laser at $\lambda = 488$ nm, in resonance with the ^5D absorption band of Tb^{3+} ion. In a general case, the refractive index change (Δn) detected by the Z-scan method may have electronic and thermal contributions. In the case of cw Z-scan measurements, the slow electronic contribution (~milliseconds) should originate from the dopant ion nonlinearity.[18,19,22] Consequently, no electronic

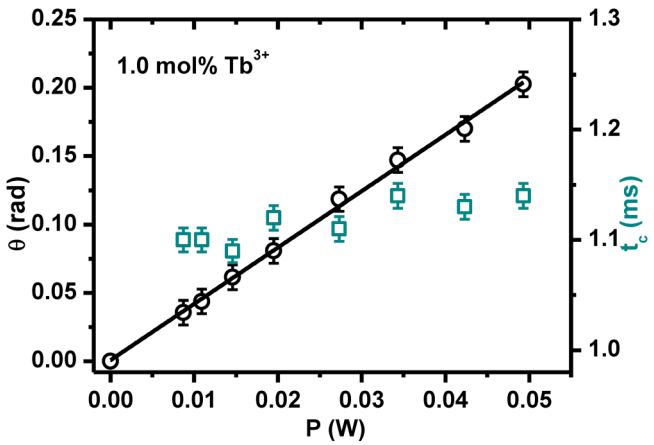

FIG. 8. Power dependence of TL parameters, θ and t_c for the 1.0 mol. % Tb doped glass.

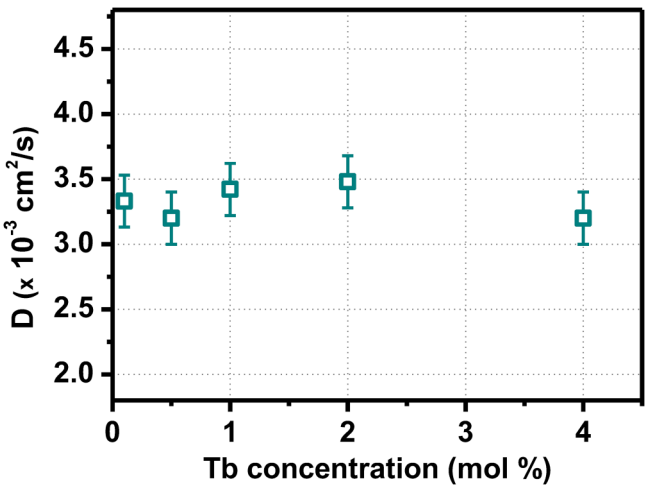

FIG. 9. Tb^{3+} concentration dependency in the thermal diffusivity (D).

signal is expected for the undoped sample. Therefore, assuming that the signal shown in Fig. 10(a) is only thermal, the data fit indicated $\theta = 0.20$ in good agreement with data shown in Fig. 8. Details about the procedure to analyze Z-scan measurements in the presence of both thermal and electronic effects can be found in Refs. 31 and 32, which presents a theoretical expression for the Z-scan curve $\Delta T(x,t)$ in terms of the parameters θ and $\Delta\Phi_o$. In fact, the Z-scan curve obtained for the 1% doped sample [Fig. 10(b)] has an amplitude of ~10% higher than the undoped sample [Fig. 10(a)]. This difference can be attributed to the electronic effect. So, the fitting of the data in Fig. 10(b) using the same θ/P_{abs} of the undoped sample results in $\Delta\Phi_o = 0.021$. So, the electronic contribution results in $n_2' \approx 1\times10^{-10}$ cm^2/W from which the polarizability difference $\Delta\alpha_p \approx 4\times10^{-26}$ cm^3 is obtained.[19] Actually, these values related to the electronic effect are only a rough estimation since the thermal contribution is approximately one order of magnitude larger than the electronic one. Moreover, the thermal response time $t_c = w_e^2/4D \sim 360\,\mu$s is comparable to response time of the electronic contribution, which is the fluorescence lifetime ~490 μs. In this case, time-resolved discrimination of thermal and electronic effects is not useful, as demonstrated in Cr^{3+} and Nd^{3+} doped fluoride.[22]

Figure 11 shows an interesting observation done by monitoring the green fluorescence, detected by a photodiode, along the Z-scan measurement. Figure 11(a) compares the transient fluorescence signal in the focus ($z = 0$) with the signal far from this point (at $z = 1.5$ cm). The decrease of the signal near focus position can be attributed to a luminescence saturation mechanism. Since the luminescence intensity is directly proportional to the excited state population, it should be given by

$$Lum \propto \frac{\langle I\rangle/I_s}{1+\langle I\rangle/I_s}, \tag{5}$$

where $I = P/(\pi w^2)$ is the mean pump intensity and $I_s = h\nu_e/\sigma\tau$ is pump saturation intensity, where $h\nu_e$ is the energy of excitation

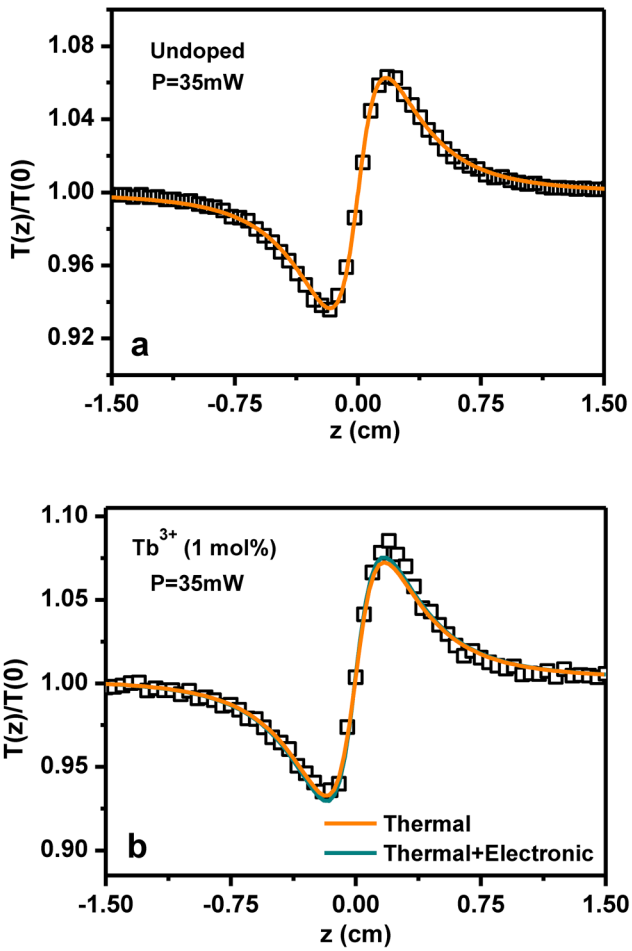

FIG. 10. Closed aperture signals, (a) undoped and (b) 1 mol. % Tb^{3+}-doped glasses under $P = 35$ mW excitation power. Open square is experimental data, and continuous line is theoretical fitting.

photon, σ is the absorption cross section, and τ is the metastable excited state lifetime. It should be noticed that in the Z-scan experiment, the excitation power is constant along the z curve, but the on-axis intensity increases near $z = 0$. In the absence of saturation, the total luminescence would remain constant along z. Figure 11(b) shows a luminescence decrease of 30% at the beam focal position. From Eq. (5), this variation provides a pump saturation intensity $I_s \sim 30$ kW/cm^2, which is approximately 80 times lower than the expected value calculated using the absorption cross section $\sigma = 3.9\times10^{-22}$ cm^2 and $\tau = 490\,\mu$s.

The saturation behavior of the green luminescence of Tb^{3+} was previously observed several glasses and crystals.[2,9] It should be noticed that the $^7F_6 \rightarrow {}^5D_4$ transition is very weak since it is dipole and spin forbidden. However, ESA from the $^5D_4$ state can reach the 4f5d levels (dipole allowed transitions) or the host matrix absorption. A detailed rate equation analysis shows that when the cross section due to ESA is much larger than the

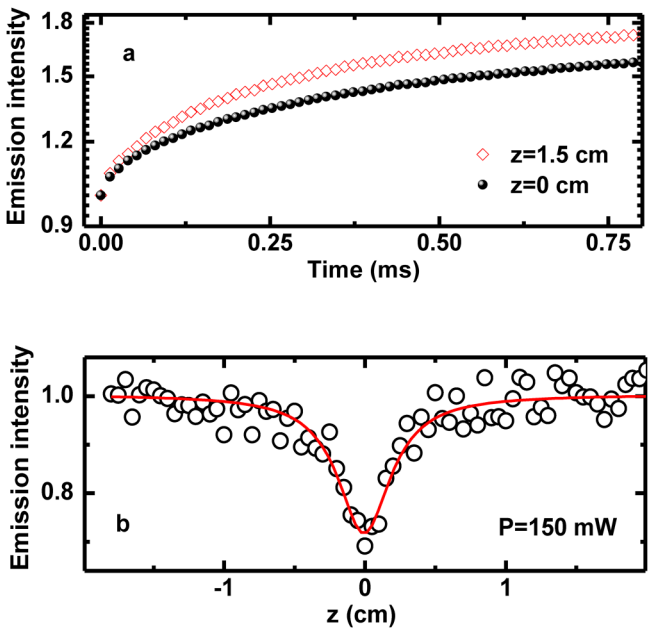

FIG. 11. (a) Transients of the fluorescence intensity in two different positions. (b) Luminescence intensity of 1 mol. % Tb^{3+}-doped glass under $P = 150$ mW excitation power for different positions through the beam path. Symbols are experimental data, and continuous line is a guide for the eyes.

ground state ($\sigma_{esa} \gg \sigma$) then the effective pump saturation intensity is given by $I_s = h\nu_e/\sigma_{esa}\tau$.[2,3] Therefore, the fluorescence saturation behavior is similar to that observed in previous experiments in Tb^{3+} doped glasses.[9]

IV. CONCLUSION

In summary, we have reported a photothermal and spectroscopic characterization of tungsten–zirconium–tellurite glass doped with several concentrations of Tb^{3+}. Absorption, excitation, and luminescence spectra showed the incorporation of the rare-earth ion in the matrix. The Tb^{3+} characteristic absorption transition $^7F_6 \rightarrow {}^5D_4$ was observed, differently of $^7F_6 \rightarrow {}^5D_3$, which was overlapped by the matrix absorption band. The majority of the luminescence spectra are related to $^5D_4$ level decay. From fluorescence decay curves, a concentration quenching was achieved for the 545 nm green emission with a critical Tb^{3+} concentration of 6.2×10^{20} cm^3 (2.7 mol. %). Thermal diffusivity ($D \sim 3.2\times10^{-3}$ cm^2/s) and optical path temperature coefficient ($ds/dT \sim 2.5\times10^{-5}$ K^{-1}) were accessed by thermal lens technique. The energy transfer efficiency from the host matrix to the Tb^{3+} was estimated from excitation spectra as ~3%, in agreement with TL measurements indicating that nearly all absorbed energy is converted into heat ($\varphi \sim 1$) for 488 nm excitation ($^7F_6 \rightarrow {}^5D_4$). This also agrees with Z-scan measurements in the cw regime, in which the achievement of nonlinear refractive index parameters was hampered due to the dominant thermal contribution. However, a saturation behavior was observed by monitoring the Tb^{3+} fluorescence along the Z-scan measurements. This effect was attributed to a strong excited state absorption as observed in other Tb^{3+} doped glasses.

ACKNOWLEDGMENTS

This work was financially supported by the Brazilian Agencies Capes and FAPESP.

REFERENCES

[1]M. J. F. Digonnet, *Rare-Earth-Doped Fiber Lasers and Amplifiers* (CRC Press, New York, 2001).
[2]J. F. M. Dos Santos, I. A. A. Terra, N. G. C. Astrath, F. B. Guimarães, M. L. Baesso, L. A. O. Nunes, and T. Catunda, "Mechanisms of optical losses in the 5D4 and 5D3 levels in Tb^{3+}doped low silica calcium aluminosilicate glasses," J. Appl. Phys. **117**, 0–8 (2015).
[3]J. F. M. dos Santos, N. G. C. Astrath, M. L. Baesso, L. A. O. Nunes, and T. Catunda, "The effect of silica content on the luminescence properties of Tb^{3+}-doped calcium aluminosilicate glasses," J. Lumin. **202**, 363–369 (2018).
[4]C. R. Kesavulu, A. C. Almeida Silva, M. R. Dousti, N. O. Dantas, A. S. S. De Camargo, and T. Catunda, "Concentration effect on the spectroscopic behavior of Tb^{3+} ions in zinc phosphate glasses," J. Lumin. **165**, 77–84 (2015).
[5]A. D. Sontakke, K. Biswas, and K. Annapurna, "Concentration-dependent luminescence of Tb^{3+} ions in high calcium aluminosilicate glasses," J. Lumin. **129**, 1347–1355 (2009).
[6]T. O. Sales, R. J. Amjad, C. Jacinto, and M. R. Dousti, "Concentration dependent luminescence and cross-relaxation energy transfers in Tb^{3+} doped fluoroborate glasses," J. Lumin. **205**, 282–286 (2019).
[7]N. Abdellaoui, F. Starecki, C. Boussard-Pledel, Y. Shpotyuk, J.-L. Doualan, A. Braud, E. Baudet, P. Nemec, F. Cheviré, M. Dussauze, B. Bureau, P. Camy, and V. Nazabal, "Tb^{3+} doped Ga5Ge20Sb10Se65-xTex (x = 0-375) chalcogenide glasses and fibers for MWIR and LWIR emissions," Opt. Mater. Express **8**, 2887 (2018).
[8]P. W. Metz, D.-T. Marzahl, A. Majid, C. Kränkel, and G. Huber, "Efficient continuous wave laser operation of Tb^{3+}-doped fluoride crystals in the green and yellow spectral regions," Laser Photon. Rev. **10**, 335–344 (2016).
[9]T. Yamashita and Y. Ohishi, "Amplification and lasing characteristics of Tb^{3+}-doped fluoride fiber in the 0.54 μm band," Jpn. J. Appl. Phys. **46**, L991–L993 (2007).
[10]G. S. Bianchi, V. S. Zanuto, F. B. G. Astrath, L. C. Malacarne, I. A. A. Terra, T. Catunda, L. A. O. Nunes, C. Jacinto, L. H. C. Andrade, S. M. Lima, M. L. Baesso, and N. G. C. Astrath, "Resonant excited state absorption and relaxation mechanisms in Tb^{3+}-doped calcium aluminosilicate glasses an investigation by thermal mirror spectroscopy," Opt. Lett. **38**, 4667 (2013).
[11]T. Schweizer, P. E.-A. Möbert, J. R. Hector, D. W. Hewak, W. S. Brocklesby, D. N. Payne, and G. Huber, "Optical measurement of narrow band rare-earth 4f levels with energies greater than the band gap of the host," Phys. Rev. Lett. **80**, 1537–1540 (1998).
[12]G. Boudebs, S. Cherukulappurath, H. Leblond, J. Troles, F. Smektala, and F. Sanchez, "Experimental and theoretical study of higher-order nonlinearities in chalcogenide glasses," Opt. Commun. **219**, 427–433 (2003).
[13]S. M. Lima, A. S. S. De Camargo, L. A. O. Nunes, T. Catunda, and D. W. Hewak, "Fluorescence quantum efficiency measurements of excitation and nonradiative deexcitation processes of rare earth 4f-states in chalcogenide glasses," Appl. Phys. Lett. **81**, 589–591 (2002).
[14]A. K. Rufino Souza, A. P. Langaro, J. R. Silva, F. B. Costa, K. Yukimitu, J. C. Silos Moraes, L. Antonio de Oliveira Nunes, L. Humberto da Cunha Andrade, and S. M. Lima, "On the efficient $Te^{4+}\rightarrow Yb^{3+}$ cooperative energy transfer mechanism in tellurite glasses: A potential material for luminescent solar concentrators," J. Alloys Compd. **781**, 1119–1126 (2019).
[15]F. A. Santos, M. S. Figueiredo, E. C. Barbano, L. Misoguti, S. M. Lima, L. H. C. Andrade, K. Yukimitu, and J. C. S. Moraes, "Influence of lattice

modifier on the nonlinear refractive index of tellurite glass," Ceram. Int. **43**, 15201–15204 (2017).
[16]L. Moreira, R. F. Falci, H. Darabian, V. Anjos, M. J. V. Bell, L. R. P. Kassab, C. D. S. Bordon, J. L. Doualan, P. Camy, and R. Moncorgé, "The effect of excitation intensity variation and silver nanoparticle codoping on nonlinear optical properties of mixed tellurite and zinc oxide glass doped with Nd2O3 studied through ultrafast z-scan spectroscopy," Opt. Mater. **79**, 397–402 (2018).
[17]R. C. Powell, S. A. Payne, L. L. Chase, and G. D. Wilke, "Four-wave mixing of Nd^{3+}-doped crystals and glasses," Phys. Rev. B **41**, 8593–8602 (1990).
[18]S. M. Lima and T. Catunda, "Discrimination of resonant and nonresonant contributions to the nonlinear refraction spectroscopy of ion-doped solids," Phys. Rev. Lett. **99**, 1–4 (2007).
[19]T. A. Vieira, J. F. M. dos Santos, Y. M. Auad, L. A. O. Nunes, N. G. Astrath, M. L. Baesso, and T. Catunda, "Pump-induced refractive index changes in Tb^{3+} doped glasses," J. Lumin. **169**, 659–664 (2016).
[20]A. Ródenas, C. Jacinto, L. R. Freitas, D. Jaque, and T. Catunda, "Nonlinear refraction and absorption through phase transition in a Nd:SBN laser crystal," Phys. Rev. B **79**, 1–4 (2009).
[21]C. R. Kesavulu, K. Suresh, J. F. M. dos Santos, T. Catunda, H. J. Kim, and C. K. Jayasankar, "Spectroscopic investigations of 1.06 μm emission and time resolved Z-scan studies in Nd^{3+}-doped zinc tellurite based glasses," J. Lumin. **192**, 1047–1055 (2017).
[22]C. Jacinto, D. N. Messias, A. A. Andrade, S. M. Lima, M. L. Baesso, and T. Catunda, "Thermal lens and Z-scan measurements: Thermal and optical properties of laser glasses—A review," J. Non-Cryst. Solids **352**, 3582–3597 (2006).
[23]T. S. Gonçalves, J. F. M. dos Santos, L. F. Sciuti, T. Catunda, and A. S. S. de Camargo, "Thermo-optical spectroscopic investigation of new Nd^{3+}-doped fluoro-aluminophosphate glasses," J. Alloys Compd. **732**, 887–893 (2018).
[24]V. Pilla, P. R. Impinnisi, and T. Catunda, "Measurement of saturation intensities in ion doped solids by transient nonlinear refraction," Appl. Phys. Lett. **70**, 817–819 (1997).
[25]T. Yamashita and Y. Ohishi, "Concentration and temperature effects on the spectroscopic properties of Tb^{3+}doped borosilicate glasses," J. Appl. Phys. **102**, 123107 (2007).
[26]V. K. Rai, S. B. Rai, and D. K. Rai, "Optical properties of Tb^{3+} doped tellurite glass," J. Mater. Sci. **39**, 4971–4975 (2004).
[27]L. A. Florêncio, L. A. Gómez-Malagón, B. C. Lima, A. S. L. Gomes, J. A. M. Garcia, and L. R. P. Kassab, "Efficiency enhancement in solar cells using photon down-conversion in Tb/Yb-doped tellurite glass," Sol. Energy Mater. Sol. Cells **157**, 468–475 (2016).
[28]A. D. Sontakke and K. Annapurna, "Study on Tb^{3+} containing high silica and low silica calcium aluminate glasses: Impact of optical basicity," Spectrochim. Acta Part A Mol. Biomol. Spectrosc. **94**, 180–185 (2012).
[29]V. Pilla, "Thermo-optical properties and nonradiative quantum efficiency of Er^{3+}-doped and Er^{3+}/Tm^{3+}-co-doped tellurite glasses," J. Non-Cryst. Solids **352**, 3598–3602 (2006).
[30]M. Seshadri, M. Radha, H. Darabian, L. C. Barbosa, M. J. V. Bell, and V. Anjos, "Thermal and nonlinear optical properties of Tm^{3+}-doped tellurite glasses," J. Therm. Anal. Calorim. **138**, 2971–2978 (2019).
[31]A. A. Andrade, E. Tenório, T. Catunda, M. L. Baesso, A. Cassanho, and H. P. Jenssen, "Discrimination between electronic and thermal contributions to the nonlinear refractive index of SrAlF_5:Cr^{+3}," J. Opt. Soc. Am. B **16**, 395 (1999).
[32]L. R. Freitas, C. Jacinto, A. Ródenas, D. Jaque, and T. Catunda, "Time-resolved study electronic and thermal contributions to the nonlinear refractive index of Nd^{3+}:SBN laser crystals," J. Lumin. **128**, 1013–1015 (2008).